Effects of flow fluctuations and partial thermalization on v_4

Clément Gombeaud[1] and Jean-Yves Ollitrault[1]

[1] *CNRS, URA2306, IPhT, Institut de physique theorique de Saclay, F-91191 Gif-sur-Yvette, France*

(Dated: July 27, 2009)

The second and fourth Fourier harmonic of the azimuthal distribution of particles, v_2 and v_4, have been measured in Au+Au collisions at the Relativistic Heavy Ion Collider (RHIC). The ratio $v_4/(v_2)^2$ is significantly larger than predicted by hydrodynamics. Effects of partial thermalization are estimated on the basis of a transport calculation, and are shown to increase $v_4/(v_2)^2$ by a small amount. We argue that the large value of $v_4/(v_2)^2$ seen experimentally is mostly due to elliptic flow fluctations. However, the standard model of eccentricity fluctuations is unable to explain the large magnitude of $v_4/(v_2)^2$ in central collisions.

PACS numbers: 25.75.Ld, 24.10.Nz

I. INTRODUCTION

The azimuthal distribution of particles emitted in ultrarelativistic nucleus-nucleus collisions at RHIC is a sensitive tool in understanding the bulk properties of the matter produced in these collisions (see [1] for a recent review). It is generally written as a Fourier series

$$\frac{dN}{d\phi} \propto 1 + 2v_2 \cos 2\phi + 2v_4 \cos 4\phi + \cdots \qquad (1)$$

where ϕ is the azimuthal angle with respect to the direction of flow. In this paper, we consider analyses done near the center-of-mass rapidity, so that odd harmonics vanish by symmetry. The large magnitude of elliptic flow, v_2, suggests that the lump of matter formed in a Au-Au collision at RHIC is close to local thermal equilibrium and expands as a relativistic fluid. Elliptic flow is large at high p_t (up to 0.25 for baryons), which motivated the idea to study the higher-order harmonic v_4 [2]. Several analyses of v_4 have been reported [3, 4, 5, 6]. Experimental results give $v_4 \simeq (v_2)^2$, while the ideal-fluid picture generally predicts $v_4 = (v_2)^2/2$ [7]. This discrepancy has not yet been explained. In this paper, we investigate the sensitivity of v_4 to two effects: viscous deviations from the ideal-fluid picture (Sec. III), and elliptic flow fluctuations (Sec. V).

II. IDEAL HYDRODYNAMICS

We first briefly recall the prediction of relativistic hydrodynamics. In this theory, the ϕ dependence of particle distribution results from a similar ϕ dependence of the fluid 4-velocity [8]:

$$u(\phi) = U\left(1 + 2V_2 \cos 2\phi + 2V_4 \cos 4\phi \cdots\right), \qquad (2)$$

where ϕ is the azimuthal angle of the fluid velocity with respect to the minor axis of the participant ellipse [10] (see Fig. 1). This is due to the fact that the overlap area between the two colliding nuclei is elliptic, which results in anisotropic pressure gradients. For a semi-central Au-Au collision at RHIC, $V_2 \sim 4\%$, and one expects V_4 to be of much smaller magnitude, typically $V_4 \sim (V_2)^2$.

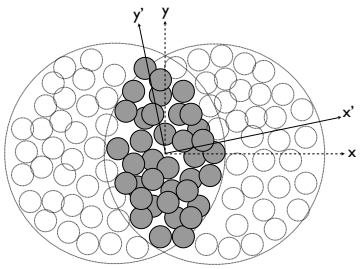

FIG. 1: Schematic picture of a nucleus-nucleus collision depicted in the transverse plane (from [9]). The principal axes (x' and y') of the area formed by the participants are tilted with respect to the reaction plane given by the axes (x and y) of the transverse plane.

The fluid expands, becomes dilute and eventually transforms into particles. As argued in Ref. [7], fast particles are produced where the fluid velocity is maximum, and parallel to the particle momentum. The resulting momentum distribution is a boosted thermal distribution. Neglecting quantum statistics (this is justified in the transverse momentum range where v_4 is measured), the momentum distribution for a given particle of mass m is

$$\frac{dN}{p_t dp_t d\phi} \propto e^{-p\cdot u/T} = \exp\left(-\frac{m_t u_0(\phi) - p_t u(\phi)}{T}\right), \quad (3)$$

where $m_t = \sqrt{p_t^2 + m^2}$, $u_0(\phi) = \sqrt{1 + u(\phi)^2}$, and ϕ is the azimuthal angle of the particle. Inserting Eq. (2) into Eq. (3), expanding to leading order in V_2, V_4 and identifying with Eq. (1), one obtains [7]

$$\begin{aligned} v_2(p_t) &= \frac{V_2 U}{T}\left(p_t - m_t v\right) \\ v_4(p_t) &= \frac{1}{2} v_2(p_t)^2 + \frac{V_4 U}{T}\left(p_t - m_t v\right), \end{aligned} \qquad (4)$$

where $v \equiv U/\sqrt{1+U^2}$. The higher harmonic v_4 is the sum of two contributions: an "intrinsic" v_4 proportional

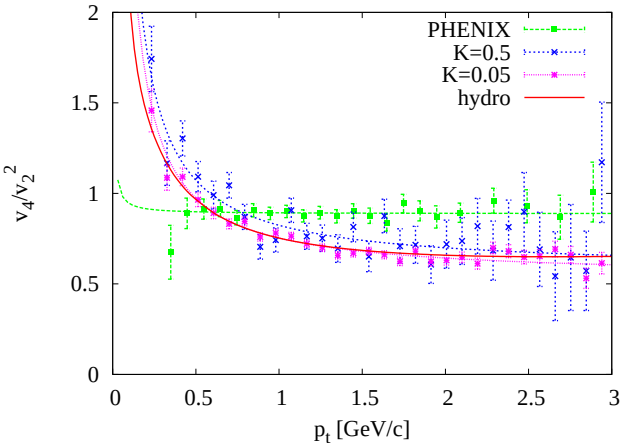

FIG. 2: (Color online) $v_4/(v_2)^2$ versus p_t in Boltzmann transport theory and ideal hydrodynamics for massless particles. Solid lines are 2-parameter fits using Eq. (5) over the interval $[0.5, 2.5]$ GeV/c. The curves are labeled by the value of the Knudsen number K. Error bars are statistical. The square dots are results for charged pions from PHENIX [6], averaged over the centrality interval 20-60%.

to the $\cos 4\phi$ term in the fluid velocity distribution, V_4, and a contribution induced by elliptic flow itself, which turns out to be exactly $\frac{1}{2}(v_2)^2$. The latter contribution becomes dominant as p_t increases. Note that if v_2 scales like the initial eccentricity of the overlap area, ϵ, v_4 scales like ϵ^2 rather than with a higher-order eccentricity ϵ_4, as assumed in Ref. [11].

In order to confirm these qualitative results, we solve numerically the equations of ideal relativistic hydrodynamics. The fluid is initially at rest. We choose a gaussian initial entropy density profile, with rms widths $\sigma_x = 2$ fm and $\sigma_y = 3$ fm. The equation of state is that of an two-dimensional ideal gas of massless particles, $s \propto T^2$, for reasons to be explained below. The normalization has been fixed in such a way that the average transverse momentum per particle is $\langle p_t \rangle = 0.42$ GeV/c, which is roughly the value for pions in a central Au-Au collision at RHIC [12]. Fig. 2 displays the variation of $v_4/(v_2)^2$ with the particle transverse momentum p_t. For massless particles, $m_t = p_t$ and Eq. (4) gives $v_4/(v_2)^2 = 0.5 + k/p_t$, where k is independent of p_t. To check the validity of this formula, our numerical results are fitted over the interval $0.5 < p_t < 2.5$ GeV/c by the simple formula

$$\frac{v_4(p_t)}{v_2(p_t)^2} = A + B\frac{\langle p_t \rangle}{p_t}, \tag{5}$$

where we have introduced the average transverse momentum $\langle p_t \rangle$ in such a way that the coefficient B is dimensionless. We refer to A (resp. B) as to the induced (resp. intrinsic) v_4. We find $A = 0.557$ and $B = 0.479$. The value of A is close to the expected value 0.5. The small discrepancy is due to the fact that Eqs. (4) are only valid for small values of v_2 and v_4. This approximation breaks down at the upper end of our fitting interval, where $v_2(2.5 \text{ GeV}/c) = 0.51$. For large p_t, however, the intrinsic V_4 term in Eq. (4) can be neglected, because it is linear in p_t while the other term is quadratic in p_t. Neglecting this term, the Fourier expansion in Eq. (1) can be done exactly. This yields

$$v_{2n}(p_t) = \frac{I_n(x)}{I_0(x)}, \tag{6}$$

where $x = 2V_2U(p_t - m_t v)/T$, and $I_n(x)$ is the modified Bessel function. Inverting Eq. (6) with $n = 1$ and $v_2 = 0.51$, one obtains $x = 1.19$. Eq. (6) with $n = 2$ then gives $v_4/(v_2)^2 = 0.552$, in better agreement with our numerical result.

We have systematically investigated the sensitivity of our hydrodynamical results to initial conditions. With a smaller initial excentricity ($\sigma_x = 2$ fm and $\sigma_y = 2.5$ fm), the value of A is closer to 0.5, as expected from the discussion above. We have also repeated the calculation with a more realistic density profile corresponding to a Au-Au collision at RHIC, obtained using an optical Glauber model calculation. We expected that B, which we understand as the "intrinsic" v_4, would be sensitive to the change in initial conditions, but the changes in both A and B were insignificant.

Experimental results are also shown in Fig. 2. A fit to these results using Eq. (5) gives $B = 0.01 \pm 0.04$, compatible with 0: the intrinsic v_4 is negligible.[1] The other fit parameter is $A = 0.89 \pm 0.02$, significantly larger than the value 0.5 predicted by hydrodynamics. Some of the discrepancies between our model calculation and data can be attributed to the equation of state, which is much softer in QCD near the transition region than in our hydrodynamical calculation. More specifically, the coefficient B representing the intrinsic v_4 may depend on the equation of state. It would be interesting to investigate this sensitivity in future hydrodynamical calculations. On the other hand, our argument leading to $A = \frac{1}{2}$ is quite general, so that the discrepancy with data cannot be attributed to the equation of state. In this paper, we investigate the possible origins of this discrepancy.

III. PARTIAL THERMALIZATION

It has been argued [14] that if interactions among the produced particles are not strong enough to produce local thermal equilibrium, so that the hydrodynamic description breaks down, the resulting value of $v_4/(v_2)^2$ is higher. This is confirmed by transport calculations within the AMPT model [15]. We investigate systematically the magnitude of this effect by solving numerically

[1] Note, however, that STAR results for charged particles [13] clearly display an intrinsic v_4 component, although smaller than in our calculation.

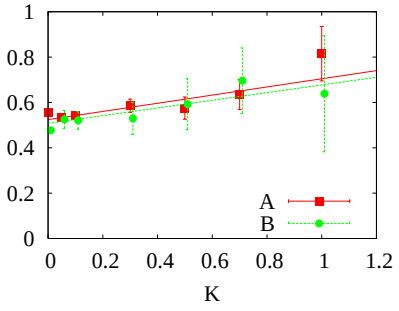

FIG. 3: (Color online) Variation of the dimensionless fit parameters A and B from Eq. (5) with the Knudsen number K. Error bars are statistical. Lines are linear fits. The points at $K = 0$ are obtained from an independent hydrodynamical calculation and are excluded from the fit.

a relativistic Boltzmann equation, where the mean free path λ of the particles can be tuned by varying the elastic scatting cross section σ. The degree of thermalization is characterized by the Knudsen number

$$K = \frac{\lambda}{R}, \tag{7}$$

where R is a measure of the system size. We consider massless particles moving in the transverse plane (no longitudinal motion) [16]. In the limit $K \to 0$, this Boltzmann equation is expected to be equivalent to ideal hydrodynamics, with the equation of state of a two-dimensional ideal gas. For sake of consistency with our hydrodynamical calculation, the initial phase space distribution of particles is locally thermal: $dN/d^2x d^2p_t \propto \exp(-p_t/T(x,y))$, where the temperature profile $T(x,y)$ is the same as in the hydrodynamical calculation. The Knudsen number is normalized as in Ref. [16]:

$$K = \frac{4\pi\sqrt{\sigma_x^2 + \sigma_y^2}}{N\sigma}, \tag{8}$$

where N is the total number of particles in the Monte-Carlo simulation, and σ the scattering cross section, which has the dimension of a length in two dimensions. Fig. 2 displays our results for two values of K. The results for $K = 0.05$ are almost identical to the results from ideal hydrodynamics, as expected. For $K = 0.5$, $v_4/(v_2)^2$ is larger, as anticipated in Ref. [14]. Although the fit formula (5) is inspired by hydrodynamics, the quality of the fit is equally good for the Boltzmann calculation. In particular, the ratio $v_4/(v_2)^2$ quickly saturates with increasing p_t, which means that the scaling $v_4 \propto (v_2)^2$ still holds if the system does not reach local thermal equilibrium, as already observed in previous transport calculations [19].

The sensitivity of v_4 to the Knudsen number K is seen more clearly in Fig. 3, which displays the variation of the fit parameters A and B with K. A linear extrapolation of our Boltzmann results to the limit $K = 0$ gives $A = 0.524 \pm 0.008$ and $B = 0.508 \pm 0.012$, to be compared

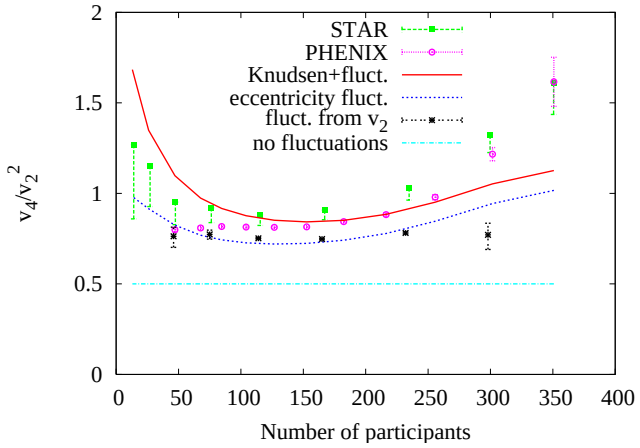

FIG. 4: (Color online) Results from STAR [20] and PHENIX [21] for charged hadrons produced in Au-Au collisions at 200 GeV/c per nucleon pair, versus the number of participant nucleons. We have averaged the ratios $v_4/(v_2)^2$ over the intervals $1.0 < p_t < 2.7$ GeV/c for STAR, $1.0 < p_t < 2.4$ GeV/c for PHENIX. Dash-dotted line: prediction from ideal hydrodynamics without flow fluctuations. Stars: with fluctuations inferred from the difference between $v_2\{2\}$ and $v_2\{\mathrm{LYZ}\}$ (Sec. V A) . Dashed line: with eccentricity fluctuations (Sec. V B). Full line: eccentricity fluctuations+partial thermalization.

with our results from ideal hydrodynamics $A = 0.557$ and $B = 0.479$, in good agreement[2].

These transport results may be sensitive to the choice of initial conditions. We have assumed a locally thermal momentum distribution. Now, the prediction $v_4/(v_2)^2$ from hydrodynamics originates precisely from the assumption that momentum distributions are thermal in the rest frame of the fluid, see Eq. (3). Replacing the exponential in this equation with a more general function $f(p\cdot u)$ leads to $v_4/(v_2)^2 = ff''/(2f'^2)$. With a power law distribution $f(x) = (1+x/x_0)^{-\alpha}$, the value of $v_4/(v_2)^2$ is enhanced by a factor $(1+\alpha)/\alpha$. Values of α inferred from p_t spectra are in the range 7-10 [17], which leads to a very slight deviation from the prediction of hydrodynamics.

Realistic values of the Knudsen number K, inferred from the centrality dependence of v_2 [18], are in the range $0.3 - 0.5$ for semi-central collisions. For these values, Fig. 3 shows that $v_4/(v_2)^2$ is at most 0.6, still significantly below the experimental value 0.9. We conclude that partial thermalization alone cannot explain experimental data.

[2] There is a small residual discrepancy of a few percent between Boltzmann and ideal hydrodynamics, which we do not understand.

IV. CENTRALITY DEPENDENCE OF $v_4/(v_2)^2$

RHIC experiments have analyzed in detail the centrality dependence of $v_4/(v_2)^2$. Preliminary results from STAR [20] and PHENIX [21] are presented in Fig. 4. The values of $v_4/(v_2)^2$ are larger than 0.8 for all centralities, and increase up to 1.6 for central collisions. Both experiments observe a similar centrality dependence of $v_4/(v_2)^2$. STAR obtains values slightly higher than PHENIX. This difference may be due to nonflow effects, which are smaller for PHENIX than for STAR because the reaction plane detector is in a different rapidity window than the central arm detector [6]. Nonflow effects contribute both to v_2 and v_4. We now estimate the order of magnitude of the error on v_4. We consider for simplicity the case when v_4 is analyzed from three-particle correlations. The corresponding estimate of v_4, denoted by $v_4\{3\}$ [22], is defined by

$$v_4\{3\} \equiv \frac{\langle \cos(4\phi_1 - 2\phi_2 - 2\phi_3)\rangle}{(v_2)^2} \tag{9}$$

where ϕ_j are azimuthal angles of outgoing particles and angular brackets denote an average over triplets of particles belonging to the same event. In Eq. (9), v_2 must be obtained from another analysis. Nonflow effects arise when particles 1 and 2 come from the same source [3]. Assuming that the source flows with the same v_2 as the daughter particles, we obtain

$$\langle \cos(4\phi_1 - 2\phi_2 - 2\phi_3)\rangle = v_4(v_2)^2 + \delta_{\rm nf}(v_2)^2, \tag{10}$$

where $\delta_{\rm nf}$ is the nonflow correlation. The latter can be estimated [23] using the azimuthal correlation δ_{pp} measured in proton-proton collisions [24] and scaling it down by the number of participants: $\delta_{\rm nf} = 2\delta_{pp}/N_{\rm part}$. Dividing by $(v_2)^4$, we obtain the corresponding error on $v_4/(v_2)^2$:

$$\delta\left(\frac{v_4}{(v_2)^2}\right)_{\rm nf} = \frac{2\delta_{pp}}{N_{\rm part}(v_2)^2}. \tag{11}$$

In practice, the analysis is done using the event-plane method rather than three-particle correlations, but this changes little the magnitude of nonflow effects [23]. The error (11) varies with centrality like $1/\chi^2$, where $\chi \sim v_2\sqrt{N}$ is the resolution parameter entering the flow analysis. The numerical value $\delta_{pp} = 0.0145$ has been used in Ref. [23] to subtract nonflow effects from v_2. It was obtained by integrating the azimuthal correlation in proton-proton collisions over p_t. The error bar on STAR results in Fig. 4 is obtained using Eq. (11) with $\delta_{pp} = 0.0145$. The agreement with PHENIX is much improved. However, this may be a coincidence: in the case of v_4, which is measured at relatively large p_t, nonflow effects are likely to be larger; on the other hand, nonflow contributions to v_2 tend to increase v_2 and decrease the ratio $v_4/(v_2)^2$, which goes in the opposite direction. Finally, we must keep in mind that even with a rapidity gap as in the PHENIX analysis, there may be a residual nonflow error of a similar magnitude.

V. FLOW FLUCTUATIONS

The scaling $v_4 = 0.5\ (v_2)^2$ predicted by ideal hydrodynamics only holds for identified particles at a given transverse momentum p_t and rapidity y, for a given initial geometry. In order to increase the statistics, however, experimental results for v_2 and v_4 are averaged over some of these quantities *before* computing the ratio $v_4/(v_2)^2$. The averaging process increases the ratio. For instance, the results shown in Fig. 2 are averaged over a large centrality interval 20-60%. Even within a narrow centrality class, the initial geometry varies significantly due to fluctuations in the initial state [25, 26] We now discuss the influence of these fluctuations on v_2 and v_4. We assume for simplicity that v_2 and v_4 are analyzed using two-particle correlations and three-particle correlations, respectively. The case where the analysis is done using the event-plane method is more complex and will be discussed in Sec. VI. The estimate of v_2 from two-particle correlations is denoted by $v_2\{2\}$ and defined by $v_2\{2\}^2 \equiv \langle\cos(2\phi_1 - 2\phi_2)\rangle$. If v_2 fluctuates within the sample of events, $\langle\cos(2\phi_1 - 2\phi_2)\rangle = \langle(v_2)^2\rangle$. Similarly, if v_4 and v_2 fluctuate, $\langle\cos(4\phi_1 - 2\phi_2 - 2\phi_3)\rangle = \langle v_4(v_2)^2\rangle$. We thus obtain

$$\frac{v_4\{3\}}{v_2\{2\}^2} = \frac{\langle v_4(v_2)^2\rangle}{\langle(v_2)^2\rangle^2} = \frac{1}{2}\frac{\langle(v_2)^4\rangle}{\langle(v_2)^2\rangle^2}, \tag{12}$$

where, in the last equality, we have assumed that the prediction of hydrodynamics $v_4 = (v_2)^2/2$ holds for a given value of v_2. If v_2 fluctuates, $\langle(v_2)^4\rangle > \langle(v_2)^2\rangle^2$, which shows that elliptic flow fluctuations increase the observed $v_4/(v_2)^2$. We now estimate quantitatively the magnitude of these fluctuations.

A. Flow fluctuations from v_2 analyses

The magnitude of v_2 fluctuations can be inferred from the difference between estimates of v_2, which is dominated by flow fluctuations except for very peripheral collisions [23]. The estimate from 2-particle correlations, $v_2\{2\}$, gives directly $\langle(v_2)^2\rangle$, while the estimate of v_2 from 4-particle cumulants, denoted by $v_2\{4\}$, involves $\langle(v_2)^4\rangle$ [27]:

$$v_2\{4\}^4 \equiv 2\left\langle(v_2)^2\right\rangle^2 - \left\langle(v_2)^4\right\rangle. \tag{13}$$

Inverting this relation, one obtains

$$\frac{\left\langle(v_2)^4\right\rangle}{\left\langle(v_2)^2\right\rangle^2} = 2 - \left(\frac{v_2\{4\}}{v_2\{2\}}\right)^4. \tag{14}$$

Inserting this equation into Eq. (12), one obtains an estimate of the effect of v_2 fluctuations on v_4. We use $v\{2\}$ from [28]; instead of $v_2\{4\}$, we use the more recent measurement $v_2\{\mathrm{LYZ}\}$ using Lee-Yang zeroes [29, 30], which

is expected to have a similar sensitivity to flow fluctuations. Data on $v_2\{\mathrm{LYZ}\}$ are only available for semi-central collisions. The resulting prediction for $v_4/(v_2)^2$ is shown in Fig. 4. The agreement with data is much improved when fluctuations are taken into account.

B. Flow fluctuations from eccentricity fluctuations

Since there are no data on $v_2\{\mathrm{LYZ}\}$ for the most central and peripheral bins, we need a model of v_2 fluctuations to cover the whole centrality range. We use the standard model of eccentricity fluctuations [10, 27], where v_2 scales like the initial eccentricity of the overlap area between the nuclei (see Fig. 1). This eccentricity is the sum of two terms:

$$\epsilon = |\epsilon_s(b)\vec{e}_x + \vec{\epsilon}^*|\,, \tag{15}$$

where $\epsilon_s(b)$ is the "standard" eccentricity at impact parameter b, computed using an average density profile, and $\vec{\epsilon}^* = (\epsilon_x^*, \epsilon_y^*)$ is a random fluctuation in the transverse plane, which is gaussian to a good approximation [31]:

$$\frac{dN}{d\epsilon_x^* d\epsilon_y^*} = \frac{1}{\pi\sigma_0^2}\exp\left(-\frac{\epsilon_x^{*2}+\epsilon_y^{*2}}{\sigma_0^2}\right). \tag{16}$$

We take the simple Ansatz $\sigma_0 = 2N_{\mathrm{part}}^{-1/2}$ [32], where N_{part} is the number of participant nucleons. As for the standard eccentricity, we assume that the initial density scales like the density of participants, which is estimated using an optical Glauber calculation [33]. Using Eqs. (15) and (16), one obtains

$$\frac{\langle (v_2)^4\rangle}{\langle (v_2)^2\rangle^2} = \frac{\langle \epsilon^4\rangle}{\langle \epsilon^2\rangle^2} = \frac{\langle \epsilon_s^4\rangle + 4\langle \epsilon_s^2\rangle \sigma_0^2 + 2\sigma_0^4}{(\langle \epsilon_s^2\rangle + \sigma_0^2)^2} \tag{17}$$

where $\langle \epsilon_s^2\rangle$ and $\langle \epsilon_s^4\rangle$ are evaluated using the distribution of impact parameter within the centrality class. For a perfectly central collision, ϵ_s vanishes, and Eqs. (12) and (17) show that flow fluctuations increase $v_4/(v_2)^2$ by a factor 2.

Experimentally, PHENIX determines the centrality using a beam-beam counter (BBC). We assume that the energy in the BBC has a gaussian distribution for a fixed impact parameter, where the mean of the gaussian and the square width scale like the number of participants [33]. Inserting Eq. (17) into Eq. (12), we obtain an estimate of the effect of eccentricity fluctuations on v_4. Our results are presented in Fig. 4. For semi-central collisions, the estimate is in good agreement with the estimate from the difference between v_2 analyses, which can be accounted for by eccentricity fluctuations [23]. For the most central bin, however, eccentricity fluctuations only increase $v_4/(v_2)^2$ by a factor 2, while a factor 3 would be needed to match STAR and PHENIX data. We have repeated the calculation by computing ϵ_s from the color-glass condensate [34]. We then need to increase the magnitude of σ_0 by 25% in order to reproduce the difference between $v_2\{2\}$ and $v_2\{4\}$. Eventually, the changes in $v_4/(v_2)^2$ are insensitive.

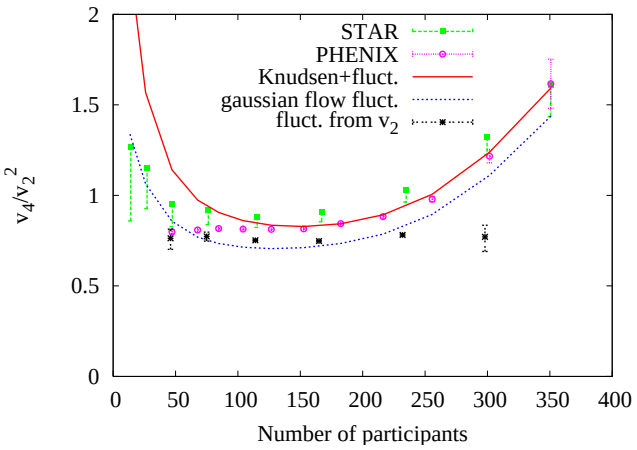

FIG. 5: (Color online) Results using a toy model of gaussian v_2 fluctuations. STAR and PHENIX data as in Fig. 4. Dashed line: ideal hydrodynamics+gaussian flow fluctuations. Full line: gaussian flow fluctuations and partial thermalization.

We now combine the effects of flow fluctuations and partial thermalization, discussed in Sec. III. We take partial thermalization into account using the linear fit to the coefficient A from Fig. 3:

$$\frac{v_4}{(v_2)^2} = \frac{1}{2} + 0.18\ K. \tag{18}$$

This modifies Eq. (12) into the following equation:

$$\frac{v_4\{3\}}{v_2\{2\}^2} = \left(\frac{1}{2} + 0.18\ K\right)\frac{\langle (v_2)^4\rangle}{\langle (v_2)^2\rangle^2}. \tag{19}$$

We borrow the estimate of K from Ref. [18]. Results are shown in Fig. 4. Partial thermalization is a small effect. It increases significantly the agreement with data for semicentral collisions, not for central collisions. For peripheral collisions, it overshoots PHENIX data.

C. A toy model of Gaussian flow fluctuations

In order to illustrate the sensitivity of v_4 to the statistics of v_2 fluctuations, we finally consider a toy model where the distribution of v_2 at fixed impact parameter b is Gaussian:

$$\frac{dN}{dv_2} = \frac{1}{\sigma_v\sqrt{2\pi}}\exp\left(-\frac{(v_2-\kappa\epsilon_s(b))^2}{2\sigma_v^2}\right). \tag{20}$$

We assume that σ_v scales like $N_{\mathrm{part}}^{-1/2}$, as generally expected for initial state fluctuations, and we adjust the proportionality constant so as to match the difference between $v_2\{2\}$ and $v_2\{4\}$. The result is displayed in Fig. 5. For semicentral and peripheral collisions, this model is

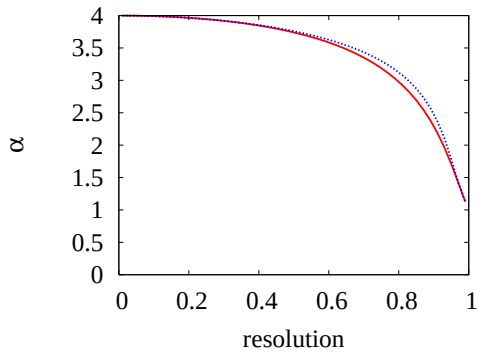

FIG. 6: Effect of fluctuations on $v_4\{\mathrm{EP}\}/v_2\{\mathrm{EP}\}^2$. The parameter α, defined in Eq. (22), is plotted versus the resolution of the event-plane for elliptic flow. The solid curve is the usual case where the event-plane consists of two subevents; the dotted curve is the case where the event-plane consists of only one subevent [9].

essentially equivalent to the standard model of eccentricity fluctuations, because the width has been adjusted to match v_2 fluctuations. For central collisions, however, results are very different, because one-dimensional gaussian fluctuations satisfy $\left\langle (v_2)^4 \right\rangle / \left\langle (v_2)^2 \right\rangle^2 = 3$ for central collisions, instead of 2 for eccentricity fluctuations, which are two-dimensional. The toy model is in very good agreement with data once partial thermalization is taken into account using Eq. (19). However, it lacks theoretical foundations: we do not know any microscopic picture that would produce such gaussian fluctuations.

VI. FLUCTUATIONS AND FLOW METHODS

In practice, v_2 and v_4 are analyzed using the event-plane method [35, 36]. The corresponding estimates are denoted by $v_2\{\mathrm{EP}\}$ and $v_4\{\mathrm{EP}\}$. In this Section, we argue that flow fluctuations have almost the same effect on $v_4\{\mathrm{EP}\}$ as on $v_4\{3\}$. We limit our study to small fluctuations for simplicity, in the same spirit as in Ref. [23]. We write $v_2 = \langle v_2 \rangle + \delta v$, with $\langle \delta v \rangle = 0$ and $\langle \delta v^2 \rangle = \sigma_v^2$, where σ_v characterizes the magnitude of flow fluctuations. Expanding Eq. (12) to leading order in σ_v, we obtain

$$\frac{v_4\{3\}}{v_2\{2\}^2} = \frac{1}{2}\left(1 + 4\frac{\sigma_v^2}{\langle v_2 \rangle^2}\right). \tag{21}$$

Similarly, one can write

$$\frac{v_4\{\mathrm{EP}\}}{v_2\{\mathrm{EP}\}^2} = \frac{1}{2}\left(1 + \alpha\frac{\sigma_v^2}{\langle v_2 \rangle^2}\right), \tag{22}$$

where α depends on the reaction plane resolution. A similar parametrization has been introduced for the fluctuations of $v_2\{\mathrm{EP}\}$ [9]. The expression of α is derived in Appendix A using the same methods as in Ref. [23]. Fig. 6 displays the variation of α with the event-plane resolution for elliptic flow. One sees that $\alpha < 4$, which means that the effect of fluctuations is always smaller for $v_4\{\mathrm{EP}\}$ than for $v_4\{3\}$; this is confirmed by the experimental observation $v_4\{3\} > v_4\{\mathrm{EP}\}$ [3]. The resolution is 1 when the reaction plane is reconstructed exactly. In this limit, $v_2\{\mathrm{EP}\} = \langle v_2 \rangle$, $v_4\{\mathrm{EP}\} = \frac{1}{2}\langle (v_2)^2 \rangle$, which implies $\alpha = 1$. In practice, however, the maximum resolution for mid-central collisions is 0.84 for STAR [28] and 0.74 for PHENIX [6]. In the case of PHENIX, α is larger than 3.2 for all centralities, which means that the effect of fluctuations is decreased at most by 20% compared to our estimates in the previous section.

VII. DISCUSSION

We have shown that experimental data on v_4 are rather well explained by combining the prediction $v_4 = (v_2)^2/2$ from hydrodynamics with elliptic flow fluctuations. If this scenario is correct, then $v_4/(v_2)^2$ should be independent of particle species and rapidity for fixed p_t and centrality. This is confirmed by preliminary results from PHENIX, which give the same value for pions, kaons and protons [6]. Note that our scenario does not support the picture of hadron formation through quark coalescence at large p_t [37]. Indeed, quark coalescence requires that $v_4/(v_2)^2$ for the underlying quark distribution is around 2, significantly larger than the observed $v_4/(v_2)^2$ for hadrons [38]. Now, the model calculation presented in this paper is below the data for hadrons; the discrepancy would be much worse with the underlying quark distribution.

The centrality dependence of v_4 offers a sensitive probe of the mechanism underlying flow fluctuations. Eccentricity fluctuations have been shown to explain quantitatively v_2 data in Au-Au and Cu-Cu collisions. We find that they also explain most of the results on v_4 for peripheral and semi-central collisions. However, they are unable to explain the steep rise of $v_4/(v_2)^2$ for the most central bins, which is clearly seen both by STAR and PHENIX. Data suggest that $\left\langle (v_2)^4 \right\rangle / \left\langle (v_2)^2 \right\rangle^2 \simeq 3$ for the most central bin, while eccentricity fluctuations give 2. We cannot exclude a priori that this is due to large errors in the extraction of v_4: if we multiply the nonflow error estimated in Sec. IV by a factor 4, data agree with our calculation for central collisions; however, the agreement is spoilt for peripheral collisions. It therefore seems unlikely that the discrepancy is solely due to nonflow effects. These results suggest that initial state fluctuations do not reduce to eccentricity fluctuations, as recently shown by a study of transverse momentum fluctuations [39]. Interestingly, the direct measurement of v_2 fluctuations attempted by PHOBOS [40], which agrees with the prediction from eccentricity fluctuations, does not extend to the most central bin.

An independent confirmation that $\left\langle (v_2)^4 \right\rangle / \left\langle (v_2)^2 \right\rangle^2 \simeq 3$ for central collisions could be obtained from the 4-particle cumulant analysis. Interestingly, there is no

published value of $v_2\{4\}$ for the most central bin: the reason is probably that $v_2\{4\}$ cannot be defined using Eq. (13), because the right-hand side is negative. This indicates that $\langle (v_2)^4 \rangle / \langle (v_2)^2 \rangle^2 > 2$. It would be interesting to repeat the cumulant analysis for central collisions, and to scale the right-hand side of Eq. (13) by $v_2\{2\}^4$. The ratio should be around -1 if $\langle (v_2)^4 \rangle / \langle (v_2)^2 \rangle^2 \simeq 3$. This would give invaluable information on the mechanism driving elliptic flow fluctuations.

APPENDIX A: EFFECT OF FLUCTUATIONS ON THE EVENT-PLANE v_4

In this Appendix, we derive the expression of α in Eq. (22). This parameter measures the effect of fluctuations on $v_4/(v_2)^2$ when flow is analyzed using the event-plane method. The event plane v_4 is defined by

$$v_4\{\mathrm{EP}\} \equiv \frac{\langle \cos 4(\phi - \Psi_R) \rangle}{R_4}, \tag{A1}$$

where ϕ is the azimuthal angle of the particle, Ψ_R is the angle of the event plane, and R_4 is the event-plane resolution in the fourth harmonic. Using Eq. (A1), the relative variation of $v_4/(v_2)^2$ due to eccentricity fluctuations can be decomposed as the sum of three contributions

$$\frac{\delta(v_4/(v_2)^2)}{(v_4/(v_2)^2)} = \frac{\delta\langle \cos 4(\phi - \Psi_R) \rangle}{\langle \cos 4(\phi - \Psi_R) \rangle} - \frac{\delta R_4}{R_4} - 2\frac{\delta v_2}{v_2}. \tag{A2}$$

The first term on the right-hand side is the contribution of fluctuations to the correlation with the event plane, the second term is the contribution of fluctuations to the resolution, the last term is the contribution of fluctuations to $v_2\{\mathrm{EP}\}$. The definition of α, Eq. (22), can be rewritten as

$$\frac{\delta(v_4/(v_2)^2)}{(v_4/(v_2)^2)} = \frac{\sigma_v^2}{\langle v_2 \rangle^2}\alpha. \tag{A3}$$

The three terms in Eq. (A2) give additive contributions to α, which we evaluate in turn.

We start with the correlation with the event-plane. The event plane Ψ_R is determined from elliptic flow [35]. Even flow harmonics v_{2n} are analyzed by correlating particles with this event plane: $\langle \cos 2n(\phi - \Psi_R) \rangle = v_{2n}\mathcal{R}_{2n}(\chi)$, where the resolution $\mathcal{R}_{2n}$ is given by [36]

$$\mathcal{R}_{2n}(\chi) = \frac{\sqrt{\pi}}{2} e^{-\chi^2/2} \chi \left(I_{\frac{n-1}{2}}\left(\frac{\chi^2}{2}\right) + I_{\frac{n+1}{2}}\left(\frac{\chi^2}{2}\right) \right), \tag{A4}$$

where χ is the resolution parameter, which is estimated using the correlation between two subevents. For $n = 2$, this equation reduces to

$$\mathcal{R}_4(\chi) = \frac{e^{-\chi^2} - 1 + \chi^2}{\chi^2}. \tag{A5}$$

These relations are derived neglecting flow fluctuations. If v_2 fluctuates, the resolution parameter χ scales like v_2, $\chi = r v_2$. Assuming in addition that v_4 scales like $(v_2)^2$, the relative change due to fluctuations is, to leading order in σ_v,

$$\begin{aligned} \frac{\delta\langle \cos 4(\phi - \Psi_R) \rangle}{\langle \cos 4(\phi - \Psi_R) \rangle} &= \frac{\sigma_v^2}{2} \frac{\frac{d^2}{(dv_2)^2}\left((v_2)^2 \mathcal{R}_4(r v_2)\right)}{\langle v_2 \rangle^2 \mathcal{R}_4(r\langle v_2 \rangle)} \\ &= \frac{\sigma_v^2}{2\langle v_2 \rangle^2} \frac{\frac{d^2}{d\chi^2}\left(\chi^2 \mathcal{R}_4(\chi)\right)}{\mathcal{R}_4(\chi)}, \end{aligned} \tag{A6}$$

where the right-hand side is evaluated for $\chi \equiv r\langle v_2 \rangle$, the average resolution parameter. Using Eq. (A5), one obtains

$$\frac{1}{\mathcal{R}_4(\chi)} \frac{d^2}{d\chi^2}\left(\chi^2 \mathcal{R}_4(\chi)\right) = \frac{2\chi^2(e^{\chi^2} + 2\chi^2 - 1)}{1 + e^{\chi^2}(\chi^2 - 1)}. \tag{A7}$$

Inserting into Eqs. (A6) and (A2), and identifying with Eq. (A3), we obtain the contribution to α from the correlation with the event plane:

$$\alpha_{\mathrm{ep}} = \frac{\chi^2(e^{\chi^2} + 2\chi^2 - 1)}{1 + e^{\chi^2}(\chi^2 - 1)}. \tag{A8}$$

We now evaluate the second term in Eq. (A2), namely, the shift in the resolution from fluctuations. The resolution is defined as $R_4 \equiv \mathcal{R}_4(\chi^{\mathrm{exp}})$, where χ^{exp} is determined from the correlation between subevents. Flow fluctuations shift the estimated resolution. Writing $\chi^{\mathrm{exp}} = \chi + \delta\chi$, one obtains, to leading order in $\delta\chi$,

$$\frac{\delta R_4}{R_4} = \frac{\chi \mathcal{R}_4'(\chi)}{\mathcal{R}_4(\chi)} \frac{\delta\chi}{\chi}. \tag{A9}$$

Eq. (A5) gives

$$\frac{\chi \mathcal{R}_4'(\chi)}{\mathcal{R}_4(\chi)} = \frac{2(e^{\chi^2} - \chi^2 - 1)}{1 + e^{\chi^2}(\chi^2 - 1)}. \tag{A10}$$

The shift in the resolution to fluctuations is given by Eq. (A7) of Ref. [23]

$$\frac{\delta\chi}{\chi} = \frac{\sigma_v^2}{2\langle v \rangle^2}\left(1 - 2\chi_s^2 + \frac{4i_1^2}{i_0^2 - i_1^2}\right). \tag{A11}$$

where $i_{0,1}$ is a shorthand notation for $I_{0,1}(\chi_s^2/2)$, and χ_s denotes the resolution parameter of a subevent. Inserting Eqs. (A10) and (A11) into (A9) and (A2), and identifying with Eq. (A3), we obtain the contribution to α from the resolution:

$$\alpha_{\mathrm{res}} = \frac{e^{\chi^2} - \chi^2 - 1}{1 + e^{\chi^2}(\chi^2 - 1)}\left(1 - 2\chi_s^2 + \frac{4i_1^2}{i_0^2 - i_1^2}\right) \tag{A12}$$

Finally, the third term in Eq. (A2) is

$$2\frac{\delta v_2}{v_2} = \frac{\sigma_v^2}{\langle v_2 \rangle^2}(\alpha_{v_2} - 1) \tag{A13}$$

where α_{v_2} is given by Eq. (23) of Ref. [23]:

$$\alpha_{v_2} = 2 - \frac{I_0 - I_1}{I_0 + I_1}\left(2\chi^2 - 2\chi_s^2 + \frac{4i_1^2}{i_0^2 - i_1^2}\right), \qquad \text{(A14)}$$

where $I_{0,1}$ is a shorthand notation for $I_{0,1}(\chi^2/2)$.

The final result is obtained by summing the three contributions from Eqs. (A8), (A12) and (A14):

$$\alpha = \alpha_{\rm ep} - \alpha_{\rm res} - (\alpha_{v_2} - 1). \qquad \text{(A15)}$$

The limit of low resolution $\chi \to 0$ (resp. high resolution $\chi \to \infty$) is $\alpha_{\rm ep} = 6$ (resp. 1), $\alpha_{\rm res} = 1$ (resp. 0), $\alpha_{v_2} = 2$ (resp. 1), $\alpha = 4$ (resp. 1).

ACKNOWLEDGMENTS

We thank Yuting Bai, Shengli Huang and Roy Lacey for sending us preliminary data from STAR and PHENIX, and Constantin Loizides for permission to use a figure of Ref. [9]. We thank François Gelis, Tuomas Lappi, Art Poskanzer and Raimond Snellings for useful discussions, and Jean-Paul Blaizot for useful comments on the manuscript.

[1] S. A. Voloshin, A. M. Poskanzer and R. Snellings, arXiv:0809.2949 [nucl-ex].
[2] P. F. Kolb, Phys. Rev. C **68**, 031902 (2003) [arXiv:nucl-th/0306081].
[3] J. Adams *et al.* [STAR Collaboration], Phys. Rev. Lett. **92**, 062301 (2004) [arXiv:nucl-ex/0310029].
[4] H. Masui [PHENIX Collaboration], Nucl. Phys. A **774**, 511 (2006) [arXiv:nucl-ex/0510018].
[5] B. I. Abelev *et al.* [the STAR Collaboration], Phys. Rev. C **75**, 054906 (2007) [arXiv:nucl-ex/0701010].
[6] S. Huang [PHENIX Collaboration], J. Phys. G **35**, 104105 (2008) [arXiv:0804.4864 [nucl-ex]].
[7] N. Borghini and J. Y. Ollitrault, Phys. Lett. B **642**, 227 (2006) [arXiv:nucl-th/0506045].
[8] P. Huovinen, P. F. Kolb, U. W. Heinz, P. V. Ruuskanen and S. A. Voloshin, Phys. Lett. B **503**, 58 (2001).
[9] B. Alver *et al.*, Phys. Rev. C **77**, 014906 (2008) [arXiv:0711.3724 [nucl-ex]].
[10] S. Manly *et al.* [PHOBOS Collaboration], Nucl. Phys. A **774**, 523 (2006) [arXiv:nucl-ex/0510031]; B. Alver *et al.* [PHOBOS Collaboration], Phys. Rev. Lett. **98**, 242302 (2007) [arXiv:nucl-ex/0610037].
[11] R. A. Lacey, A. Taranenko and R. Wei, arXiv:0905.4368 [nucl-ex].
[12] B. I. Abelev *et al.* [STAR Collaboration], Phys. Rev. C **79**, 034909 (2009) [arXiv:0808.2041 [nucl-ex]].
[13] Y. Bai [STAR Collaboration], J. Phys. G **34**, S903 (2007) [arXiv:nucl-ex/0701044].
[14] R. S. Bhalerao, J. P. Blaizot, N. Borghini and J. Y. Ollitrault, Phys. Lett. B **627**, 49 (2005) [arXiv:nucl-th/0508009].
[15] L. W. Chen, C. M. Ko and Z. W. Lin, Phys. Rev. C **69**, 031901 (2004) [arXiv:nucl-th/0312124].
[16] C. Gombeaud and J. Y. Ollitrault, Phys. Rev. C **77**, 054904 (2008) [arXiv:nucl-th/0702075].
[17] J. Adams *et al.* [STAR Collaboration], Phys. Lett. B **637**, 161 (2006) [arXiv:nucl-ex/0601033].
[18] H. J. Drescher, A. Dumitru, C. Gombeaud and J. Y. Ollitrault, Phys. Rev. C **76**, 024905 (2007) [arXiv:0704.3553 [nucl-th]].
[19] T. Z. Yan *et al.*, Phys. Lett. B **638**, 50 (2006) [arXiv:nucl-th/0605022].
[20] Yuting Bai, PhD thesis, the University of Utrecht.
[21] Roy Lacey, private communication.
[22] N. Borghini, P. M. Dinh and J. Y. Ollitrault, Phys. Rev. C **64**, 054901 (2001) [arXiv:nucl-th/0105040].
[23] J. Y. Ollitrault, A. M. Poskanzer and S. A. Voloshin, Phys. Rev. C **80**, 014904 (2009) [arXiv:0904.2315 [nucl-ex]].
[24] J. Adams *et al.* [STAR Collaboration], Phys. Rev. Lett. **93**, 252301 (2004) [arXiv:nucl-ex/0407007].
[25] C. E. Aguiar, Y. Hama, T. Kodama and T. Osada, Nucl. Phys. A **698**, 639 (2002) [arXiv:hep-ph/0106266].
[26] W. Broniowski, P. Bozek and M. Rybczynski, Phys. Rev. C **76**, 054905 (2007) [arXiv:0706.4266 [nucl-th]].
[27] M. Miller and R. Snellings, arXiv:nucl-ex/0312008.
[28] J. Adams *et al.* [STAR Collaboration], Phys. Rev. C **72**, 014904 (2005) [arXiv:nucl-ex/0409033].
[29] B. I. Abelev *et al.* [STAR Collaboration], Phys. Rev. C **77**, 054901 (2008) [arXiv:0801.3466 [nucl-ex]].
[30] R. S. Bhalerao, N. Borghini and J. Y. Ollitrault, Nucl. Phys. A **727**, 373 (2003) [arXiv:nucl-th/0310016].
[31] S. A. Voloshin, A. M. Poskanzer, A. Tang and G. Wang, Phys. Lett. B **659**, 537 (2008) [arXiv:0708.0800 [nucl-th]].
[32] R. S. Bhalerao and J. Y. Ollitrault, Phys. Lett. B **641**, 260 (2006) [arXiv:nucl-th/0607009].
[33] M. L. Miller, K. Reygers, S. J. Sanders and P. Steinberg, Ann. Rev. Nucl. Part. Sci. **57**, 205 (2007) [arXiv:nucl-ex/0701025].
[34] T. Lappi and R. Venugopalan, Phys. Rev. C **74**, 054905 (2006) [arXiv:nucl-th/0609021].
[35] A. M. Poskanzer and S. A. Voloshin, Phys. Rev. C **58**, 1671 (1998) [arXiv:nucl-ex/9805001].
[36] J. Y. Ollitrault, arXiv:nucl-ex/9711003.
[37] D. Molnar and S. A. Voloshin, Phys. Rev. Lett. **91**, 092301 (2003) [arXiv:nucl-th/0302014].
[38] P. F. Kolb, L. W. Chen, V. Greco and C. M. Ko, Phys. Rev. C **69**, 051901 (2004) [arXiv:nucl-th/0402049].
[39] W. Broniowski, M. Chojnacki and L. Obara, arXiv:0907.3216 [nucl-th].
[40] B. Alver *et al.* [PHOBOS Collaboration], arXiv:nucl-ex/0702036.